

CHEMISTRY

A European Journal



Accepted Article

Title: Selective encapsulation and separation of dihalobenzene isomers with discrete heterometallic macrocages

Authors: Guo-Xin Jin, Hai-Ning Zhang, Ye Lu, Wen-Xi Gao, and Yue-Jian Lin

This manuscript has been accepted after peer review and appears as an Accepted Article online prior to editing, proofing, and formal publication of the final Version of Record (VoR). This work is currently citable by using the Digital Object Identifier (DOI) given below. The VoR will be published online in Early View as soon as possible and may be different to this Accepted Article as a result of editing. Readers should obtain the VoR from the journal website shown below when it is published to ensure accuracy of information. The authors are responsible for the content of this Accepted Article.

To be cited as: *Chem. Eur. J.* 10.1002/chem.201805383

Link to VoR: <http://dx.doi.org/10.1002/chem.201805383>

Supported by
ACES

WILEY-VCH

Selective encapsulation and separation of dihalobenzene isomers with discrete heterometallic macrocages

Hai-Ning Zhang, Ye Lu, Wen-Xi Gao, Yue-Jian Lin and Guo-Xin Jin^{*[a,b]}

Abstract: A series of metallosupramolecular architectures have been prepared including rectangles, prisms and cages, and featuring half-sandwich rhodium(III) fragments at the vertices. Remarkably, a stable cage-like heteropolymetallic complex possessing eight rhodium(III) and two silver(I) metal ions (**3**) has been obtained following a multistep procedure. The Rh^{III}/Ag^I mixed macrocage enables the separation of dihalogenated benzene derivatives with high selectivity. Furthermore, a detailed X-ray crystallographic study confirmed that the discriminative encapsulation of *para*-dihalobenzene (dichlorobenzene, dibromobenzene and diiodobenzene) is favored by Ag- π interactions and steric effects.

Introduction

Molecular recognition, the concept was initially proposed by chemists and biologists to explore chemical problems in biological systems in the molecular level and well utilized to describe effective and selective biological function, which can also be regarded as the process forming the crucial part of self-assembly in the essence.^[1,2] Together with most advancements in Supramolecular Chemistry, molecular recognition has been widely used to depict the process in which the host (receptor) selectively binds to the guest (substrate) and both of them together produces a particular function. As the most significant field in Supramolecular Chemistry, molecular recognition has raised more and more attentions from supramolecular chemists and further inspires them to design and synthesize molecular machines with intricate structures and various kinds of functions.^[3]

Understanding the coordination-driven self-assembly of discrete metallosupramolecular architectures can shed light on significant behavioral aspects of complicated recognition process, thus allowing major breakthroughs in supramolecular

recognition.^[4] Due to their remarkable solubility in a wide variety of solvents, self-assembled metallamacrocycles and metallacages have found application in several research areas,^[5,6] including catalysis, biosciences, separation processes and the development of advanced sensors.^[7,8]

Haloarenes are valuable starting materials for cross-coupling reactions, a key step in the synthesis of drugs and conjugated organic compounds.^[9,10] Due to their similar chemical and physical properties, traditional methods either have great difficulties in separating of haloarene isomers or effect the separation with high cost. Therefore, purification of these chemical compounds demands particular attention, both at research laboratory and large-scale industrial levels.^[11] Previously reported procedures to separate haloaromatic constitutional isomers are mainly based on the different molecular radii of these compounds and use porous materials with different pore sizes and shapes^[11] (zeolites, activated carbon, carbon molecular sieves, aluminophosphates, inorganic or polymeric resins, metal-organic frameworks and composite materials).^[12,13] However, due to unique peculiarities of these materials, most of these studies relied on computational models to explain the principles of separation rather than experimental evidence. For discrete half-sandwich iridium-, rhodium- and ruthenium-based organometallic architectures, the existence of Cp* (pentamethylcyclopentadienyl) or Cy (*para*-cymene) fragments not only improves the solubility of metallosupramolecular compounds but also facilitates their crystallization, allowing the facile determination of crystal structures of encapsulation compounds.^[5,6] These structures provide reliable evidence for the driving force of encapsulation and push forward the exploration of separation on a single-molecule level.

Herein, we report the rational and straightforward preparation of Cp*Rh-based metallosupramolecular architectures featuring stable heterarylrhodium(III) complexes *via* metal-directed self-assembly of heterocyclic boronic acids and rhodium precursors under mild conditions. Moreover, in order to realize the construction of heterometallic macrocages, the spatial regulating strategy^[4e] was adopted and three types of proligands were selected in this work (**Scheme 1**). According to the results, we found the halogen atoms not only play a crucial role in forming heterometallic macrocages, but also affect the properties of the macrocages in the separation of isomers of guest molecules and stability of encapsulation compounds. On this basis, a separation method is presented for a series of constitutional isomers of *ortho*-, *meta*- and *para*-dihalogenated benzene derivatives at ambient temperature. Thereby, the existence of bridging silver(I) ions in the cages enables reversible encapsulation and release of guest molecules by taking advantage of the well-known reduction of

[a] H.-N. Zhang, Dr. Y. Lu, W.-X. Gao, Dr. Y.-J. Lin, Prof. G.-X. Jin
State Key Laboratory of Molecular Engineering of Polymers
Collaborative Innovation Center of Chemistry for Energy Materials
Department of Chemistry, Fudan University
Shanghai 200433 (P.R. China)

[b] Prof. G.-X. Jin
State Key Laboratory of Organometallic Chemistry
Shanghai Institute of Organic Chemistry
Chinese Academy of Sciences
Shanghai 200032 (P. R. China)
E-mail: gxjin@fudan.edu.cn

Supporting information and the ORCID identification number(s) for the author(s) of this article can be found under:
<https://doi.org/10.1002/chem.XXXXXX>.

FULL PAPER

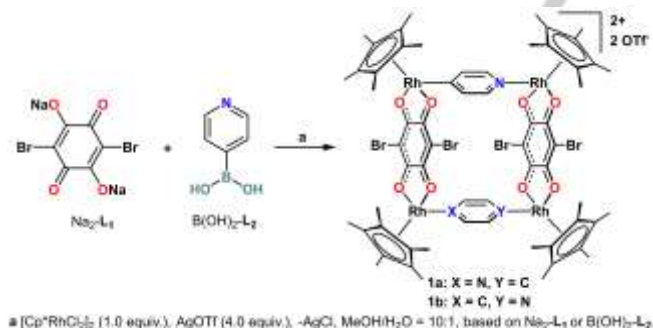
silver(I) ions under sunlight, or the reaction of silver(I) and chloride ions under mild conditions.



Scheme 1. Selected proligands with distinct coordination modes and two N-heterocyclic boronic acids.

Results and Discussion

The proligand 2,5-dibromo-3,6-dihydroxycyclohexa-2,5-diene-1,4-dione (H_2-L_1) and 2,5-difluoro-3,6-dihydroxycyclohexa-2,5-diene-1,4-dione (H_2-L_4) were synthesized according to the literature method.^[15a,15c] The ligands $B(OH)_2-L_2$: pyridine-4-boronic acid, $B(OH)_2-L_3$: pyrimidine-5-boronic acid) and proligand 2,5-dihydroxycyclohexa-2,5-diene-1,4-dione (H_2-L_5) were purchased from commercial sources and used without purification. The ligand Na_2-L_1 was synthesized *via* the reaction of proligand H_2-L_1 (1.0 equiv.) with sodium methoxide (2.0 equiv.) in methanol at ambient temperature. Analogously, the ligands Na_2-L_4 and Na_2-L_5 were also prepared by replacing proligand H_2-L_1 with proligand H_2-L_4 and H_2-L_5 in the reaction with sodium methoxide, respectively.

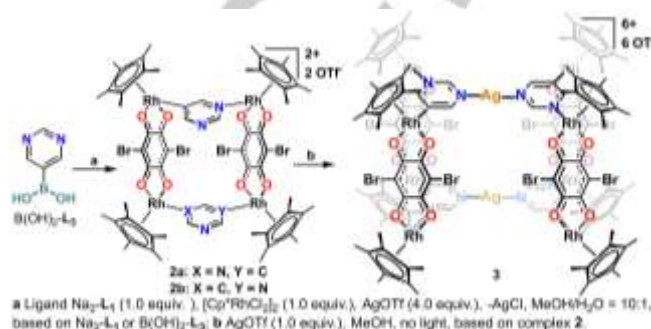


Scheme 2. Synthesis of metallarectangles 1.

Synthesis of tetranuclear rhodium metallarectangles. A methanolic solution of $[Cp^*RhCl_2]_2$ was treated with 4.0 equiv. of AgOTf (OTf = SO_3CF_3) with exclusion of light for 6 h. Subsequently, ligand Na_2-L_1 (1.0 equiv.), ligand Na_2-L_2 (1.0 equiv.) and deionized water were added to the reaction mixture. Isomeric complexes **1a** and **1b** were obtained after 24 h in a yield of 90% (**Scheme 2**).

Formation of **1a** and **1b** as isomeric mixture was unambiguously confirmed by NMR spectroscopy and single-crystal X-ray diffraction analysis. While the 1H NMR spectrum exhibited two sets of mutually coupled signals in the aromatic region at δ 7.64-6.59 ppm, the $^{13}C\{^1H\}$ NMR spectrum showed

different singlets for the carbon nuclei of the methyl groups. These features, in addition to the $^1H,^1H$ -COSY NMR spectrum, confirmed the existence of an isomeric mixture (see the Supporting Information). Furthermore, the HR-ESI mass spectrum of **1** in CH_3OH showed strong peaks at m/z 1848.74 (assigned to $[1 - OTf]^+$) and m/z 849.89 (assigned to $[1 - 2OTf]^{2+}$), indicating that complexes **1a** and **1b** exhibit remarkable stability in solution.



Scheme 3. Synthesis of metallarectangle **2** and heterometallic macrocage **3**.

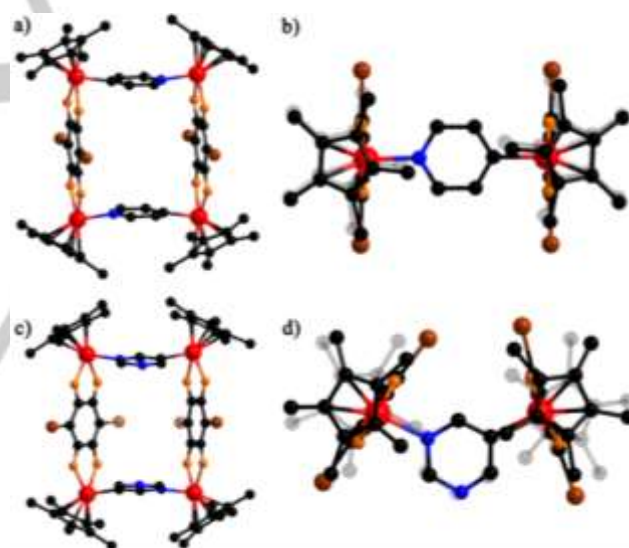


Figure 1. a) Side and b) top view of the cationic part of metallarectangle **1a**. c) Side and d) top view of metallarectangle **2a**. All triflate anions, solvent molecules, and hydrogen atoms are omitted for clarity. Color code: N, blue; O, orange; C, black; Br, brown; Rh, red.

The facile formation of metallarectangles **1a** and **1b** prompted us to investigate the related reaction involving pyrimidine-5-boronic acid ($B(OH)_2-L_3$). Since the C–B bond of $B(OH)_2-L_3$ can be easily activated by rhodium(III), as was previously observed for $B(OH)_2-L_2$, the heterocyclic boronic acid $B(OH)_2-L_3$ has three potential coordination sites. The pair of boat-shaped isomers **2a** and **2b** was obtained with a yield of 87% following a procedure similar to that introduced previously for the synthesis of **1a** and **1b** (**Scheme 3**). The mixture of tetra-Rh^{III} complexes **2a** and **2b** was

FULL PAPER

studied by ^1H NMR spectroscopy, elemental analysis and mass spectrometry. Multiple resonances were observed for the protons of the Cp^* groups in the ^1H NMR spectrum, suggesting the existence of isomers in solution and that the Cp^* groups are not chemically equivalent. Furthermore, the HR-ESI mass spectrum of **2** in CH_3OH showed strong peaks at m/z 1850.73 (assigned to $[\mathbf{2} - \text{OTf}]^+$) and m/z 850.89 (assigned to $[\mathbf{2} - 2\text{OTf}]^{2+}$), which indicates that complexes **2a** and **2b** exhibit remarkable stability in solution.

In addition, single-crystals suitable for X-ray diffraction analysis were grown by slow vapor diffusion of diethyl ether into a saturated methanolic solution of the mixture of tetranuclear rhodium metallarectangles **2a** and **2b** with a *meta*-C,N-bridging coordination mode. A remarkable feature of the structure of **2a** is that one nitrogen atom from each pyrimidinyl moiety is "bare", as demonstrated by its solid-state structure (Figure 1).

Synthesis of decanuclear heterometallic macrocages and hexanuclear prisms. In order to utilize the "bare" nitrogen atoms in complex **2**, potential coordination sites for further metal ions, silver(I) was selected to bridge two metallarectangles **2** to form a heterometallic macrocage. AgOTf (1.0 equiv.) was added with exclusion of light to a solution of **2** (1.0 equiv.) in methanol. The obtained mixture was stirred at ambient temperature to afford complex **3**. Red crystals of complex **3** were obtained in 92% yield by slow diffusion of diethyl ether into a saturated solution of **3** in methanol with exclusion of light (Scheme 3).

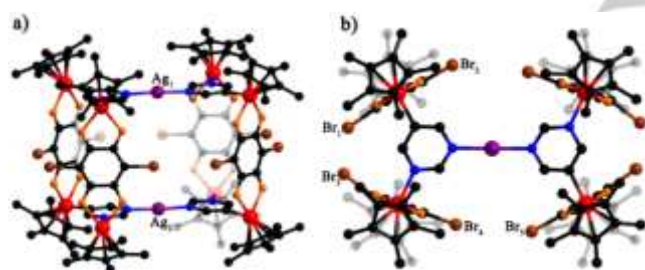


Figure 2. a) Side and b) top view of the cationic part of heterometallic macrocage **3**. All triflate anions, solvent molecules, and hydrogen atoms are omitted for clarity. Color code: N, blue; O, orange; C, black; Br, brown; Rh, red; Ag, violet. and hydrogen atoms are omitted for clarity. Color code: N, blue; O, orange; C, black; Br, brown; Rh, red.

Single-crystal X-ray crystallographic analysis of these crystals confirmed the formation of a cage-shaped heterometallic complex featuring Rh^{III} and Ag^{I} ions (Figure 2). The molecular structure of the cationic part of **3** shows the eight Rh^{III} metal centers to occupy the vertices of the metallacage. Whereas the rhodium(III) centers adopt the classical piano-stool geometry typical for half-sandwich rhodium complexes, the geometry around the silver(I) ions is best described as linear. The Ag^{I} metal centers are each bound to nitrogen atoms of two pyrimidine-5-boronic acid-derived ligands. In addition, the Cp^*Rh fragments are coordinated to both ligands L_2^- and L_3^- . The size of metallacage **3** is ca. $10.4 \times 6.1 \times 8.0$ Å ($\text{Rh} \cdots \text{Rh}$ separations), while the $\text{Ag} \cdots \text{Ag}$ distance is ca. 7.7 Å. The heteropolymetallic complex **3** was also characterized by ^1H NMR spectroscopy and elemental analysis. Since the ^1H NMR

spectra of the complex mixture **2a/2b** and **3** are different, the variations of the δ values can be attributed to the N-coordination of the metalloligands **2a** and **2b** to silver(I).

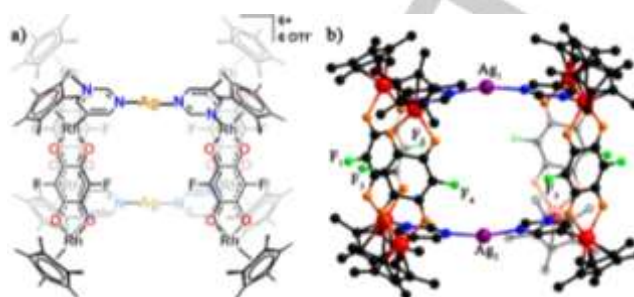
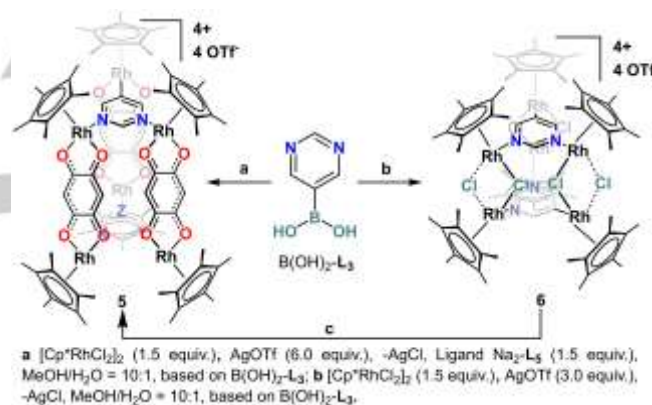


Figure 3. a) Chemical structure of heterometallic macrocage **4**; b) side view of the cationic part of heterometallic macrocage **4**. All triflate anions, solvent molecules, and hydrogen atoms are omitted for clarity. Color code: N, blue; O, orange; C, black; F, light green; Rh, red; Ag, violet.



Scheme 4. Construction of hexanuclear prisms **5** and **6**.

Furthermore, with the aim of exploring the steric effects of the ligands upon forming the heterometallic macrocages, ligands $\text{Na}_2\text{-L}_4$ and $\text{Na}_2\text{-L}_5$ were introduced into this system under conditions similar to those used for the previous frameworks. As shown in Scheme S1, the related heterometallic macrocage **4** was subsequently prepared based on ligand $\text{Na}_2\text{-L}_3$ and ligand $\text{Na}_2\text{-L}_4$ in a yield of 90% and was fully characterized by ^1H NMR spectroscopy, elemental analysis and X-ray diffraction analysis. As shown in Figure 3, the crystallographically-derived molecular structure of macrocage **4** is very similar to that of **3**, as revealed by crystallographic means. The size of metallacage **4** is ca. $10.0 \times 6.0 \times 8.0$ Å ($\text{Rh} \cdots \text{Rh}$ separations) and the measured $\text{Ag} \cdots \text{Ag}$ distance is ca. 8.7 Å.

Notably, a hexanuclear rhodium prism (**5**) was subsequently prepared *via* synthetic route in the Scheme 4 in a yield of 93% based on ligands $\text{Na}_2\text{-L}_3$ and $\text{Na}_2\text{-L}_5$ with less steric hindrance. Prism **5** was fully characterized by ^1H NMR spectroscopy, elemental analysis and X-ray diffraction analysis. Due to the poor quality of single crystals of prism **5**, its structure was roughly determined from an initially reduced structure through

FULL PAPER

crystallographic means (see the Supporting Information). Although many efforts were made to follow the synthetic methods used to prepare cages **3** and **4**, the synthesis of a macrocage based on ligand $\text{Na}_2\text{-L}_5$ was unsuccessful, which may be explained by the steric differences between the proton and fluoride or bromide groups and its effect on the structure of product. In addition, the formation of prism **5** prompted us to focus on the effect of the length of the building blocks on the structure of the resulting compounds, and an experiment based on the shorter bridging ligand $\mu\text{-Cl}$ was performed following the synthetic method used to prepare prism **5** (Scheme 4). Thereby, the smaller prism **6** was obtained in a yield of 95% and was fully characterized by ^1H NMR spectroscopy, elemental analysis and X-ray diffraction analysis. It was subsequently found that prism **6** can also serve as a precursor to prism **5**, in a yield of 96%.

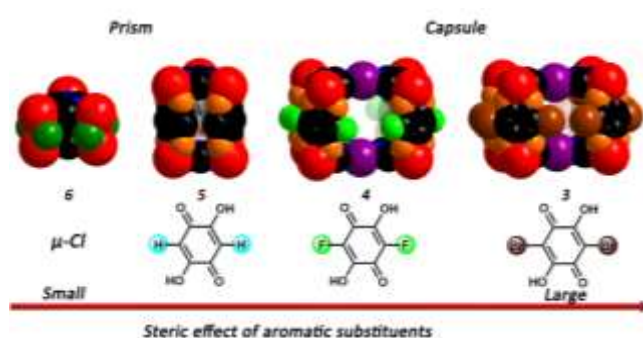


Figure 4. Space-filling representations of two prisms and two capsules. Cp^* rings, all triflate anions, solvent molecules, and hydrogen atoms are omitted for clarity. Color code: N, blue; O, orange; C, black; F, bright green; Cl, green; Br, brown; I, olive green; Ag, violet; Rh, red.

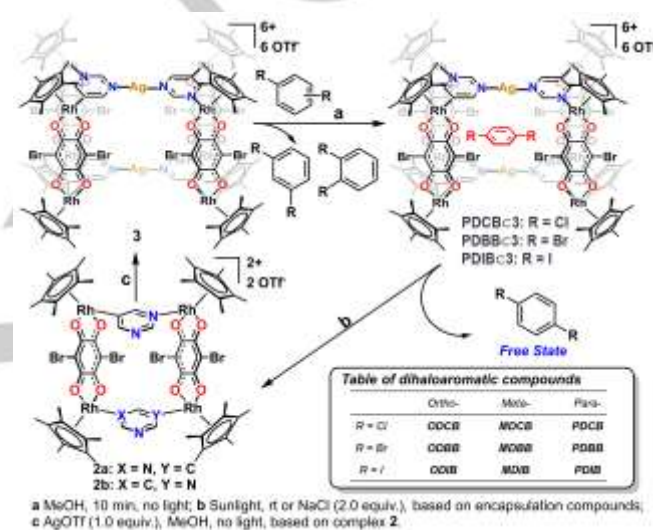
From these results in this work, it becomes clear that the substituents on aromatic ligands play a crucial role in determining the supramolecular structures of the products; *i.e.* fluoride, bromide and chloride groups lead to heterometallic macrocages while hydrogens lead to the formation of hexanuclear prism. This can be attributed to the steric effects of the substituents and further be regarded as a controllable method to prepare compounds with targeted structures (Figure 4).

Selective encapsulation of dihalobenzene derivatives.

Given the size of the cavity inside macrocages **3** and **4**, we sought to explore their host-guest properties. Therefore, we expected that varying the aromatic substituents could enable the formation of more capsules, in order to reveal their exact structures by X-ray single-crystal analysis and to effect separation of *para*-dihalobenzene derivatives. These two potential advances would help gain a better understanding the driving force of encapsulation as well as expanding the application of these heterometallic capsules in the domain of separation.

Initially, an excess of *para*-dibromobenzene (**PDBB**) was added to a saturated solution of complex **3** in CD_3OD in an NMR tube. The mixture obtained was stirred with exclusion of light at room temperature for 10 min (Scheme 5). A subsequent NMR spectroscopic analysis of the mixture revealed the appearance of

new signals belonging to free **PDBB** and an encapsulated form (**PDBB** \subset **3**). The ^1H NMR spectrum showed two singlets at δ 7.44 and 6.55 ppm, which can be attributed to the protons of **PDBB**. A comparison with the ^1H NMR spectrum of pure **PDBB** established that the singlet at δ 7.44 ppm belongs to free **PDBB** and the signal at δ 6.55 ppm belongs to **PDBB** inside the metallacage (guest state). Integration of the signals suggests that the host:guest ratio is 1:1. The encapsulation of one molecule of **PDBB** by complex **3** was subsequently confirmed with a ^1H DOSY NMR experiment involving the host-guest system **PDBB** \subset **3**. The diffusion coefficient of both the host and guest was $D = 2.67 \times 10^{-6} \text{ m}^2 \text{ s}^{-1}$. In addition, 2D EXSY experiments of a 2:1 sample of **PDBB** and empty macrocage **3** allowed determination of the exchange rate of the guests ($k \approx 2.36 \text{ s}^{-1}$).



Scheme 5. Reversible encapsulation and release of dihaloaromatic compounds with heterometallic assembly **3**.

Table 1. Selected distances (\AA) of heterometallic macrocages **3** and **4** and host-guest complexes **PDCB** \subset **3**, **PDBB** \subset **3** and **PDIB** \subset **3**.

	X^a	$\text{Ag}_1 \cdots \text{Ag}_2$	$\text{Ag}_1 \cdots \pi$	$\text{X} \cdots \pi$
Cage 4	-	8.66	-	-
Cage 3	-	7.72	-	-
PDCB \subset 3	Cl	7.50	3.37	3.76
PDBB \subset 3	Br	7.50	3.37	3.67
PDIB \subset 3	I	7.58	3.33	3.52

[a] X stands for the halogen atoms which belong to guest molecules (**PDCB**, **PDBB** and **PDIB**), respectively.

Single crystals suitable for X-ray diffraction were obtained by slow vapor diffusion of diethyl ether into a methanol solution of **PDBB** \subset **3**. Analysis of these crystals confirmed the presence of one molecule of **PDBB** inside the heterometallic macrocage **3** (Figure 5). Comparison of the metric parameters for the complex

FULL PAPER

3 and host-guest system **PDBB**⊂**3** reveals variations in bond lengths due to the encapsulation of guest **PDBB**. As shown in the Table 1, the distance between the Ag₁ and Ag₂ atoms shortens from 7.72 Å to 7.50 Å, which may be respectively induced by the Ag-π interaction between two silver atoms and one **PDBB** molecule, and the apparent Br-π interaction^[14] between the bromine atoms of **PDBB** and the plane of nearby ligand **L**₁ (Table 1). Most notably, the plane of guest molecule **PDBB** is not totally parallel to the plane containing pyrimidine and a silver(I) ion; the guest molecule exists in the host with a certain torsion angle (Figure 5). Interestingly, the N-Ag^I-N angle of **PDBB**⊂**3** is 177.0° (173.0° for complex **3**) which may be an effect of interactions between silver ions and the **PDBB** molecule. Given that **3** appeared to be of suitable size to host **PDBB** and allow formation of significant interactions between host and guest (Ag-π interaction and Br-π interaction^[14]), a detailed study of the chemical properties of **PDBB**⊂**3** was carried out, thereby indicating the high stability of the host-guest system over time in solution as well as the solid state (in the absence of ambient light).

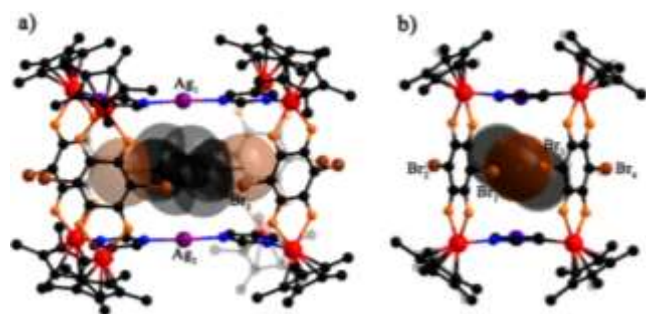


Figure 5. Side view of the cationic part of host-guest system **PDBB**⊂**3**: Ball-and-stick representation of macrocage **3** and space-filling representation of guest **PDBB**. All triflate anions, solvent molecules, and hydrogen atoms are omitted for clarity. Color code: N, blue; O, orange; C, black; Br, brown; Ag, violet; Rh, red.

Due to the successful formation of the host-guest complex **PDBB**⊂**3**, we subsequently attempted to encapsulate other dihalobenzene derivatives with metallacage **3**. *Para*-dichlorobenzene (**PDCB**) and *para*-diiodobenzene (**PDIB**) were also found to be suitable guest molecules for **3**, as confirmed by ¹H and ¹H DOSY NMR spectroscopy and X-ray diffraction analysis. The resonances corresponding to **PDCB** and **PDIB** are shifted downfield in the ¹H NMR spectra upon encapsulation of the compounds by macrocage **3**, as has been previously observed for **PDBB**. Furthermore, 2D EXSY experiments of a 2:1 sample of **PDCB** or **PDIB** and empty macrocage **3** allowed determination of the exchange rate of the guests ($k \approx 1.05 \text{ s}^{-1}$ for **PDCB**⊂**3** and $k \approx 1.88 \text{ s}^{-1}$ for **PDIB**⊂**3**).

Slow vapor diffusion of diethyl ether into a methanol solution of **PDCB**⊂**3** and **PDIB**⊂**3** yielded single crystals suitable for X-ray diffraction analysis, confirming their guest-encapsulated structures in the solid state (Figure S48). When comparing with the structure of guest-free capsule **3**, some structural changes of these two encapsulation compounds were noted, including the

shortening of the distance between the two silver atoms (induced by the Ag-π interaction between host and guest), as shown in Table 1. Additionally, halogen-π interactions between host and guest were observed in these two encapsulation compounds: the Cl-π distance is ca. 3.76 Å and I-π distance is ca. 3.52 Å (the distances are between halogen atoms and the centroid of aromatic rings), which are within the range normally found in the literature for this type of intermolecular interaction.^[14] A detailed study of the chemical properties of **PDBB**⊂**3** and **PDIB**⊂**3** was carried out, which suggested the high stability of the host-guest system over time in solution and also in the solid state (in the absence of ambient light).

The macrocage **4** was also treated with potential guest molecules **PDCB**, **PDBB** and **PDIB**; however, no obvious change was observed in the ¹H NMR spectrum of the reaction mixture, probably due to the inappropriate Ag...Ag distance (8.66 Å). Moreover, as the distance between the two proximal fluorine atoms (F₄ and F₅ atoms) becomes longer, the cavity becomes less able to form a stable encapsulated structure.

In addition, the existence of two Ag^I metal ions in **3** prompted us to study the light-induced degradation and subsequent regeneration of the cage-shaped complex. A flask containing a 10 mL solution of host-guest system **PDBB**⊂**3** in MeOH was exposed to sunlight for 8 h and this reaction mixture was filtered. The solvent amount was reduced to 1 mL under vacuum and diethyl ether was added to precipitate a red solid, which was filtered, washed with diethyl ether and dried to gain a red crystalline solid. The ¹H NMR spectrum of this red solid showed signals corresponding to the tetranuclear rhodium(III) metallarectangle **2**. AgOTf (1.0 equiv. based on **2**) and **PDBB** (0.5 equiv. based on **2**) were then added with exclusion of light to the NMR tube and the obtained mixture was stirred for 10 min, resulting in the regeneration of the host-guest system **PDBB**⊂**3**. Identical conclusions were also drawn from related experiments involving **PDCB** or **PDIB** as guest molecules. Furthermore, the addition of NaCl to an NMR tube containing a saturated solution of **PDBB**⊂**3** led to the formation of a white precipitate (AgCl), which also led to release of the guest molecules. The addition of AgOTf (1.0 equiv. based on **2**) can then form the corresponding encapsulated structures both in the solution and solid state, as confirmed by ¹H NMR spectroscopy and X-ray crystallography. In the studies of the host-guest properties of macrocage **3** and **4** described above, we were delighted to find that the interactions between guest molecules and macrocage **3** can induce structural changes, which consequently affects the selectivity for these dihaloaromatic benzene derivatives as guest molecules, as illustrated in Table 1. Considering the considerable stability of encapsulation compounds based on macrocage **3**, we selected **3** as the template for separation of *para*-dihalobenzene from mixtures of dihalobenzene isomers.

Selective encapsulation of dihalobenzene derivatives. Taking advantage of the intriguing host-guest properties of macrocage **3**, a series of constitutional isomers containing *ortho*-, *meta*- and *para*-dihalogenated benzene derivatives, such as *ortho*-dichlorobenzene (**ODCB**), *ortho*-dibromobenzene (**ODBB**), *ortho*-diiodobenzene (**ODIB**), *meta*-dichlorobenzene (**MDCB**), *meta*-dibromobenzene (**MDBB**), *meta*-diiodobenzene (**MDIB**),

FULL PAPER

para-dichlorobenzene (**PDCB**), *para*-dibromobenzene (**PDBB**) and *para*-diiodobenzene (**PDIB**), were selected to separate *para*-dihalogenated benzene derivatives from the remaining isomers under mild conditions.

Initially, reaction mixtures of experiments aimed at the selective encapsulation of dihalobenzene derivatives were monitored *via* NMR spectroscopy. After obtaining the desired result, we then immediately carried out an experiment under the larger scale in the lab. As shown in **Figure 6**, taking dibromobenzene derivatives as an example, a mixture of **ODBB**, **MDBB** and **PDBB** in *n*-hexane was added to a methanol solution of an excess of heterometallic macrocage **3**, and tetrahydrofuran (THF) was used to further precipitate **PDBB**·**3** after 10 min, leaving **ODBB** and **MDBB** in the filtrate (liquid I). Then, **PDBB** can be extracted into a new filtrate (liquid II) by leaving the methanol solution of precipitate **PDBB**·**3** under sunlight or adding NaCl (2.0 equiv., based on encapsulation compounds) and precipitating complex **2** with THF and Et₂O, as confirmed by ¹H NMR spectroscopy. Moreover, heterometallic macrocage **3** can be regenerated by

addition of AgOTf (1.0 equiv., based on complex **2**) to the methanol solution of **2**, to realize the reversible encapsulation. The structures of complex **2**, macrocage **3** and **PDBB**·**3** from this separation process were furthermore confirmed by single-crystal X-ray analysis after crystallization by comparison of their cell parameters. Subsequently, **PDCB** and **PDIB** can be respectively separated from the mixture of dichlorobenzene and diiodobenzene derivatives by adopting similar methods under ambient temperatures (**Figure 6**). Details of the experiments can be found in Experimental Section.

Furthermore, application of the above-mentioned method (**Figure 6**) allowed isolation of **PDCB** from a mixture of **PDCB**, **TRCB** (1,3,5-trichlorobenzene) and **TECB** (1,2,4,5-tetrachlorobenzene) under mild conditions. **PDBB** and **PDIB** can also be respectively separated from a mixture of **PDBB**, **TRBB** (1,3,5-tribromobenzene) and **TEBB** (1,2,4,5-tetrabromobenzene), and **PDIB** and **TRIB** (1,3,5-triiodobenzene) derivatives using a similar method.

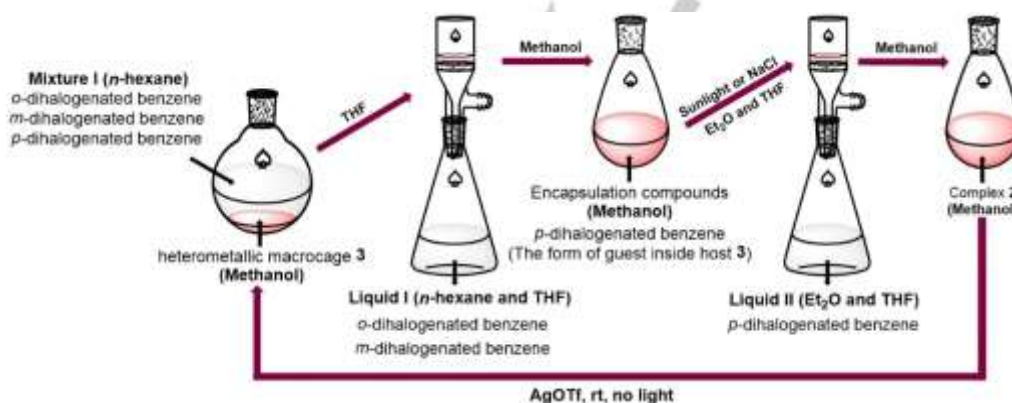


Figure 6. Method for separation of *para*-dihalogenated benzene derivatives from their isomers.

Conclusions

We have reported the construction of a series of discrete Cp*Rh-based metallocsupramolecular architectures featuring stable heteroaryl rhodium(III) units, ranging from metallarectangles to heterometallic macrocages and hexanuclear prisms, prepared by heterocyclic boronic acids and rhodium precursors under mild conditions. We then utilized the excellent host-guest abilities of these macrocages, to enable selective, reversible encapsulation of *para*-dihaloaromatic benzene derivatives and their separation from their constitutional isomers under mild conditions. We hope that these findings will promote further research into the applications of discrete heterometallic macrocages in the separation of complex mixtures, which could be useful in the separation of high-value halogenated compounds, such as isotopically labeled or radioactive derivatives.

Experimental Section

General Procedures. All mentioned reagents and solvents were purchased from commercial sources and used as supplied directly unless otherwise mentioned. The starting materials [Cp*RhCl₂]₂ and 2,5-dibromo-3,6-dihydroxycyclohexa-2,5-diene-1,4-dione were synthesized according to literature methods.^[15] 2,5-dibromo-3,6-dihydroxycyclohexa-2,5-diene-1,4-dione (H₂-L₁), 2,5-difluoro-3,6-dihydroxycyclohexa-2,5-diene-1,4-dione (H₂-L₄) and 2,5-dihydroxycyclohexa-2,5-diene-1,4-dione (H₂-L₅) were treated with sodium methoxide in methanol to obtain ligands Na₂-L₁, Na₂-L₄ and Na₂-L₅, respectively. NMR spectra were recorded on a Bruker AVANCE I 400 spectrometer. NMR spectra were recorded at room temperature and referenced to the residual protonated solvent. Proton chemical shifts are reported relative to the solvent residual peak (δ H = 3.31 for CD₃OD). Coupling constants are expressed in Hertz. Elemental analyses were performed on an Elemental Vario EL III analyzer. ESI-MS spectra were recorded on a Micro TOF II mass spectrometer. Adequate ¹³C NMR spectra of these compounds could not be obtained even after 24

FULL PAPER

h due to their limited solubility in CD₃OD.

Preparation of complex 1. A 30 mL methanol solution of [Cp*RhCl₂]₂ (1.0 equiv., 61.8 mg, 0.1 mmol) was treated with AgOTf (OTf = SO₃CF₃, 4.0 equiv., 102.3 mg, 0.4 mmol) in the dark for 6 h, followed by the addition of ligand Na₂-L₁ (1.0 equiv., 34.0 mg, 0.1 mmol), ligand B(OH)₂-L₂ (1.0 equiv., 12.3 mg, 0.1 mmol) and deionized water (2 mL), and this reaction mixture was stirred in the dark for 24 h. The solvent was evaporated under vacuum and then 5 mL methanol was added. Diethyl ether was added to precipitate the red solid, which was then filtered, washed with diethyl ether and dried to obtain a red crystalline solid. Yield: 89.9 mg, 90%. Anal. calcd for C₆₄H₆₈Br₄F₆N₂O₁₄Rh₄S₂: C, 38.46; H, 3.43; N, 1.40. Found: C, 38.50; H, 3.40; N, 1.39. ¹H NMR (400 MHz, CD₃OD, ppm): δ 7.65-7.63 (m, 4H, Py-H), 7.44-7.41 (m, 4H, Py-H), 1.65-1.60 (m, 60H, Cp*). ESI-TOF-MS: *m/z* 849.89 (calcd for [M - 2OTf]²⁺ 849.89), 1848.74 (calcd for [M - OTf]⁺ 1848.74).

Preparation of complex 2. A synthetic procedure similar to that for complex 1 was used to afford red crystalline solid complex 2, using AgOTf (102.3 mg, 0.4 mmol), [Cp*RhCl₂]₂ (61.8 mg, 0.1 mmol), ligand Na₂-L₁ (34.0 mg, 0.1 mmol) and ligand B(OH)₂-L₃ (12.4 mg, 0.1 mmol). Yield: 87.0 mg, 87%. Anal. calcd for C₆₂H₆₆Br₄F₆N₄O₁₄Rh₄S₂: C, 37.22; H, 3.33; N, 2.80. Found: C, 37.20; H, 3.36; N, 2.83. ¹H NMR (400 MHz, CD₃OD, ppm): δ 8.47 (br, 4H, Pyrim-H), 8.16 (s, 2H, Pyrim-H), 1.72-1.68 (m, 60H, Cp*). ESI-TOF-MS: *m/z* 850.89 (calcd for [M - 2OTf]²⁺ 850.89), 1850.73 (calcd for [M - OTf]⁺ 1850.73).

Preparation of complex 3. The heterometallic macrocage 3 can be prepared by two different methods:

1) AgOTf (1.0 equiv., 12.8 mg, 0.05 mmol) was added to a methanol solution of complex 2 (1.0 equiv., 100.0 mg, 0.05 mmol) and the mixture was stirred in the dark for several hours. The solvent was evaporated under vacuum and then 1 mL methanol was added. Diethyl ether was then added to precipitate the red solid, which was filtered, washed with diethyl ether and dried to obtain a red crystalline solid. Yield: 103.8 mg, 92%.

2) A 30 mL methanol solution of [Cp*RhCl₂]₂ (1.0 equiv., 61.8 mg, 0.1 mmol) was treated with AgOTf (4.0 equiv., 102.3 mg, 0.4 mmol) in the dark for 6 h, followed by the addition of ligand Na₂-L₁ (1.0 equiv., 34.0 mg, 0.1 mmol), ligand B(OH)₂-L₃ (1.0 equiv., 12.4 mg, 0.1 mmol), AgOTf (0.5 equiv., 12.8 mg, 0.05 mmol) and deionized water (2 mL), and this reaction mixture was stirred in the dark for 24 h. The solvent was evaporated under vacuum and then 5 mL methanol was added. Diethyl ether was then added to precipitate the red solid, which was filtered, washed with diethyl ether and dried to obtain a red crystalline solid. Yield: 100.5 mg, 89%. Anal. calcd for C₁₂₆H₁₃₂Ag₂Br₈F₁₈N₈O₃₄Rh₈S₆: C, 33.52; H, 2.95; N, 2.48. Found: C, 33.49; H, 2.96; N, 2.50. ¹H NMR (400 MHz, CD₃OD, ppm): δ 8.72 (br, 8H, Pyrim-H), 8.26 (s, 4H, Pyrim-H), 1.77-1.72 (m, 120H, Cp*).

Preparation of complex 4. The 30 mL methanol solution of [Cp*RhCl₂]₂ (1.0 equiv., 61.8 mg, 0.1 mmol) was treated with AgOTf (4.0 equiv., 102.3 mg, 0.4 mmol) in the dark for 6 h, followed by the addition of ligand Na₂-L₄ (1.0 equiv., 22.0 mg, 0.1 mmol), ligand B(OH)₂-L₃ (1.0 equiv., 12.4 mg, 0.1 mmol), AgOTf (0.5 equiv., 12.8 mg, 0.05 mmol) and deionized water (2 mL), and this reaction mixture was stirred in the dark for 24 h. The solvent was evaporated under vacuum and then 5 mL methanol was added. Diethyl ether was then added to precipitate the red solid, which was filtered, washed with diethyl ether and dried to obtain a red crystalline solid. Yield: 90.6 mg, 90%. Anal. calcd for C₁₂₆H₁₃₂Ag₂F₂₆N₈O₃₄Rh₈S₆: C, 37.57; H, 3.30; N, 2.78. Found: C, 37.55; H, 3.28; N, 2.79. ¹H NMR (400 MHz, CD₃OD, ppm): δ 8.66 (br, 8H, Pyrim-H), 8.19 (s, 4H, Pyrim-H), 1.75-1.70 (m, 120H, Cp*).

Preparation of complex 5. A 30 mL methanol solution of [Cp*RhCl₂]₂ (1.0 equiv., 61.8 mg, 0.1 mmol) was treated with AgOTf (4.0 equiv., 102.3 mg, 0.4 mmol) in the dark for 6 h, followed by the addition of ligand Na₂-L₅ (1.0 equiv., 18.4 mg, 0.1 mmol), ligand B(OH)₂-L₃ (0.67 equiv., 8.33 mg, 0.067 mmol), and deionized water (2 mL), and this reaction mixture was

stirred. The solvent was evaporated under vacuum and then 5 mL methanol was added. Diethyl ether was then added to precipitate the red solid, which was filtered, washed with diethyl ether and dried to obtain a red crystalline solid. Yield: 80.5 mg, 93%. Anal. calcd for C₉₀H₁₀₂F₁₂N₄O₂₄Rh₆S₄: C, 41.62; H, 3.96; N, 2.16. Found: C, 41.60; H, 3.98; N, 2.13. ¹H NMR (400 MHz, CD₃OD, ppm): δ 8.33-8.28 (m, 6H, Pyrim-H), 5.57-5.48 (m, 6H, ligand L₅-H), 1.76-1.73 (m, 90H, Cp*).

Preparation of complex 6. A 30 mL methanol solution of [Cp*RhCl₂]₂ (1.0 equiv., 61.8 mg, 0.1 mmol) was treated with AgOTf (2.0 equiv., 51.2 mg, 0.2 mmol) in the dark for 6 h, followed by ligand B(OH)₂-L₃ (1.0 equiv., 12.4 mg, 0.1 mmol) and deionized water (2 mL), and this reaction mixture was stirred. The solvent was evaporated under vacuum and then 5 mL methanol was added. Diethyl ether was then added to precipitate the red solid, which was filtered, washed with diethyl ether and dried to obtain a red crystalline solid. Yield: 75.9 mg, 95%. Anal. calcd for C₇₂H₉₆Cl₆F₁₂N₄O₁₂Rh₆S₄: C, 36.09; H, 4.04; N, 2.34. Found: C, 36.11; H, 4.01; N, 2.35. ¹H NMR (400 MHz, CD₃OD, ppm): δ 8.61-8.28 (m, 4H, Pyrim-H), 8.55 (s, 2H, Pyrim-H), 1.69-1.64 (m, 90H, Cp*).

Reversible encapsulation and release of *para*-dihaloaromatic compounds with macrocage 3.

General encapsulation process: in the dark, an excess of the guest dihaloaromatic compound was added to a solution of macrocage 3 in methanol and this mixture was stirred at ambient temperature. After 24 h the resulting solution was concentrated to 1 mL under vacuum and diethyl ether was added to precipitate the red solid, which was filtered, washed with diethyl ether and dried to obtain a red crystalline solid (dihaloaromatic compound⊂3).

General release process: exposure of encapsulation compounds in 30 mL methanol solution under sunlight for 8 h, or addition of 2.0 equiv. NaCl or NH₄Cl (based on encapsulation compounds) into the methanol solution for 10 min, led to formation of mixtures containing tetranuclear metallarectangle 2 and the guest molecules. The resulting solution was then concentrated to 5 mL under vacuum and diethyl ether was added to precipitate the red solid, which was filtered, washed with diethyl ether and dried to obtain a red crystalline solid (metallarectangle 2).

General reversible process: an excess of the guest molecule (2.0 equiv. based on complex 2) and AgOTf (1.0 equiv. based on complex 2) was added to a methanol solution of complex 2 prepared in the previous step and the mixture was stirred in the dark about for 10 min. The resulting solution was then concentrated to 1 mL under vacuum and diethyl ether was added to precipitate the reddish solid, which was filtered, washed with diethyl ether and dried to obtain a red crystalline solid (dihaloaromatic compound⊂3).

Characterization details for PDCB⊂3 (7) follow. Yield: 91.8 mg, 98.5%. Anal. calcd for C₁₃₂H₁₃₆Ag₂Cl₂Br₈F₁₈N₈O₃₄Rh₈S₆: C, 34.00; H, 2.94; N, 2.40. Found: C, 34.03; H, 3.97; N, 2.38. ¹H NMR (400 MHz, CD₃OD, ppm): δ 8.73-8.52 (m, 8H, Pyrim-H), 8.45 (s, 4H, Pyrim-H), 6.75 (s, 4H, PDCB_{inside}-H), 1.77-1.74 (m, 120H, Cp*).

Characterization details for PDBB⊂3 (8) follow. Yield: 91.2 mg, 96%. Anal. calcd for C₁₃₂H₁₃₆Ag₂Br₁₀F₁₈N₈O₃₄Rh₈S₆: C, 33.37; H, 2.89; N, 2.36. Found: C, 33.35; H, 2.90; N, 2.37. ¹H NMR (400 MHz, CD₃OD, ppm): δ 8.74-8.53 (m, 8H, Pyrim-H), 8.46 (s, 4H, Pyrim-H), 6.87 (s, 4H, PDBB_{inside}-H), 1.78-1.73 (m, 120H, Cp*).

Characterization details for PDIB⊂3 (9) follow. Yield: 94.0 mg, 97%. Anal. calcd for C₁₃₂H₁₃₆Ag₂Br₈I₂F₁₈N₈O₃₄Rh₈S₆: C, 32.72; H, 2.83; N, 2.31. Found: C, 32.73; H, 2.85; N, 2.30. ¹H NMR (400 MHz, CD₃OD, ppm): δ 8.74-8.53 (m, 8H, Pyrim-H), 8.49 (s, 4H, Pyrim-H), 6.96 (s, 4H, PDIB_{inside}-H), 1.77-1.74 (m, 120H, Cp*).

Separation of *para*-dihalobenzene derivatives from their isomers with capsule 3.

General process: in the dark, a solution (20 mL) of capsule 3 (0.01 mmol/mL) in CH₃OH was added to mixture I, which consisted of *ortho*-

FULL PAPER

dihalobenzene (0.2 mmol), *meta*-dihalobenzene (0.2 mmol), and *para*-dihalobenzene (0.2 mmol) in 3 mL *n*-hexane. After being stirred at room temperature for 10 min, the solution was allowed to stand and separate into layers; the upper layer was colorless and the lower layer was deep red. The lower layer was separated by a separating funnel, and then 100 mL of THF was added to produce a deep-red precipitate, which was collected by filtration and dried. The filtrate, liquid I, contained *ortho*-dihalobenzene and *meta*-dihalobenzene. A deep-red solid was obtained in a yield of 95.1% (886.7 mg for **PDCBc3**), 96.3% (915.0 mg for **PDBBc3**) and 94.3% (916 mg for **PDIBc3**).

Leaving a 10 mL methanol solution of above-mentioned encapsulation compounds under sunlight for ca. 12 h, or addition of NaCl (0.38 mmol for **PDCBc3**, 0.39 mmol for **PDBBc3** and 0.38 mmol for **PDIBc3**) to the solution, provided deep-red solution after filtration. The 100 mL mixture of THF and Et₂O (Volume, THF/Et₂O = 1:1) was added to achieve a deep-red precipitate, which was collected by filtration and provided liquid II, containing *para*-dihalobenzene. A deep-red solid (complex **2**) was obtained in a yield of 91.4% (696 mg for **PDCBc3**), 93.7% (722 mg for **PDBBc3**) and 92.3% (703 mg for **PDIBc3**), which was based on the product in the previous step. Subsequently, AgOTf (0.35 mmol for **PDCBc3**, 0.39 mmol for **PDBBc3** and 0.35 mmol for **PDIBc3**) was added to the solution of complex **2** in the dark to form capsule **3**, which can be used in the next separation.

X-ray crystal structure analysis

Single crystals of **1**, **2**, **3**, **4**, **6**, **7**, **8** and **9** suitable for X-ray diffraction study were obtained at room temperature. X-ray intensity data of **1**, **2**, **4**, **7**, **8** and **9** were collected at 203 K on a CCD-Bruker SMART APEX system, respectively, data of **3** and **6** was collected at 173 K on a Bruker D8 VENTURE system. In these data, the disordered solvent molecules that could not be restrained properly were removed using the SQUEEZE route. The single-crystal X-ray diffraction data of **1**, **2**, **3**, **4**, **6**, **7**, **8** and **9** have been deposited in the Cambridge Crystallographic Data Centre under accession number CCDC: 1865363 (**1**), 1865364 (**2**), 1865365 (**3**), 1865366 (**4**), 1865367 (**6**), 1865368 (**7**), 1865369 (**8**) and 1865370 (**9**).

Acknowledgements

This work was supported by the National Science Foundation of China (21531002, 21720102004) and the Shanghai Science Technology Committee (13JC1400600); G.-X. Jin thanks the Alexander von Humboldt Foundation for a Humboldt Research Award.

Conflict of interest

The authors declare no conflict of interest.

Keywords: Ag- π interaction • dihalobenzene isomers • halogen- π interaction • heterometallic macrocages • selective encapsulation • separation

- [1] a) S. H. Gellman, *Chem. Rev.* **1997**, *97*, 1231; b) F.-W. Zeng, S. C. Zimmerman, *Chem. Rev.* **1997**, *97*, 1681; c) M. Kruppa, B. König, *Chem. Rev.* **2006**, *106*, 3520; d) M. Yoshikawa, K. Tharpa, Ş.-O. Dima, *Chem. Rev.* **2016**, *116*, 11500.
- [2] a) M.-L. Lehaire, R. Scopelliti, H. Piotrowski, K. Severin, *Angew. Chem. Int. Ed.* **2002**, *41*, 1419; b) Z. Grote, M.-L. Lehaire, R. Scopelliti, K. Severin, *J. Am. Chem. Soc.* **2003**, *125*, 13638; c) J. M. Lehn, *Angew. Chem. Int. Ed.* **2013**, *52*, 2836; d) J. M. Lehn, *Angew. Chem. Int. Ed.* **2015**, *54*, 3276; e) G. Cecot, B. Alameddine, S. Prior, R. de Zorzi, S. Geremia, R. Scopelliti, F. T. Fadaei, E. Solari, K. Severin, *Chem. Commun.* **2016**, *52*, 11243.
- [3] a) S. Saha, J. F. Stoddart, *Chem. Soc. Rev.*, **2007**, *36*, 77; b) C. D. Meyer, C. S. Joiner, J. F. Stoddart, *Chem. Soc. Rev.*, **2007**, *36*, 1705; c) K. Ariga, H. Ito, J. P. Hill, H. Tsukube, *Chem. Soc. Rev.*, **2012**, *41*, 5800; d) C. Heinzmann, C. Weder, L. M. de Espinosa, *Chem. Soc. Rev.*, **2016**, *45*, 342; e) Y. Bai, Q. Luo, J. Liu, *Chem. Soc. Rev.* **2016**, *45*, 2756; f) Z.-C. Liu, S. K. M. Nalluria, J. F. Stoddart, *Chem. Soc. Rev.*, **2017**, *46*, 2459.
- [4] a) S. J. Lee, W. Lin, *Acc. Chem. Res.* **2008**, *41*, 521; b) B. H. Northrop, H.-B. Yang, P. J. Stang, *Chem. Commun.* **2008**, 5896; c) E. Zangrando, M. Casanova, E. Alessio, *Chem. Rev.* **2008**, *108*, 4979; d) M. Yoshizawa, J. K. Klosterman, M. Fujita, *Angew. Chem. Int. Ed.* **2009**, *48*, 3418; e) H. Li, Z.-J. Yao, D. Liu, G.-X. Jin, *Coord. Chem. Rev.* **2015**, *293-294*, 139.
- [5] a) H. Piotrowski, G. Hilt, A. Schulz, P. Mayer, K. Polborn, K. Severin, *Chem. - Eur. J.* **2001**, *7*, 3196; b) S. Gauthier, L. Quebatte, R. Scopelliti, K. Severin, *Chem. - Eur. J.* **2004**, *10*, 2811; c) I. Saur, R. Scopelliti, K. Severin, *Chem. - Eur. J.* **2006**, *12*, 1058; d) Y.-F. Han, G.-X. Jin, *Acc. Chem. Res.* **2014**, *47*, 3571; e) Y.-F. Han, G.-X. Jin, *Chem. Soc. Rev.* **2014**, *43*, 2799; f) S.-L. Huang, G.-X. Jin, H.-K. Luo, T. S. Hor, *Chem. - Asian J.* **2015**, *10*, 24; g) S.-L. Huang, T. S. A. Hor, G.-X. Jin, *Coord. Chem. Rev.* **2017**, *333*, 1.
- [6] a) S.-L. Huang, T. S. A. Hor, G.-X. Jin, *Coord. Chem. Rev.* **2017**, *346*, 112; b) Y. Lu, Y.-X. Deng, Y.-J. Lin, Y.-F. Han, L.-H. Weng, Z.-H. Li, G.-X. Jin, *Chem. Rev.* **2017**, *3*, 110; c) Y.-Y. Zhang, W.-X. Gao, L. Lin, G.-X. Jin, *Coord. Chem. Rev.* **2017**, *344*, 323; d) Y. Lu, H.-N. Zhang, G.-X. Jin, *Acc. Chem. Res.* **2018**, *51*, 2148; e) H.-N. Zhang, W.-X. Gao, Y.-X. Deng, Y.-J. Lin, G.-X. Jin, *Chem. Commun.* **2018**, *54*, 1559.
- [7] a) M. Fujita, J. Yazaki, K. Ogura, *J. Am. Chem. Soc.* **1990**, *112*, 5645; b) B. H. Northrop, Y.-R. Zheng, K.-W. Chi, P. J. Stang, *Acc. Chem. Res.* **2009**, *42*, 1554; c) P. Jin, S. J. Dalgarno, J. L. Atwood, *Coord. Chem. Rev.* **2010**, *254*, 1760; d) R. Chakrabarty, P. S. Mukherjee, P. J. Stang, *Chem. Rev.* **2011**, *111*, 6810; e) T. R. Cook, Y.-R. Zheng, P. J. Stang, *Chem. Rev.*, **2013**, *113*, 734; f) T. R. Cook, P. J. Stang, *Chem. Rev.* **2015**, *115*, 7001; g) W.-H. Zhang, Q. Liu, J.-P. Lang, *Coord. Chem. Rev.* **2015**, *293-294*, 187.
- [8] a) W.-Y. Zhang, Y.-J. Lin, Y.-F. Han, G.-X. Jin, *J. Am. Chem. Soc.* **2016**, *138*, 10700; b) T. M. Brauer, Q. Zhang, K. Tiefenbacher, *J. Am. Chem. Soc.* **2017**, *139*, 17500; c) A. J. McConnell, C. M. Aitchison, A. B. Grommet, J. R. Nitschke, *J. Am. Chem. Soc.* **2017**, *139*, 6294; d) B. Roy, A. Devaraj, R. Saha, S. Jharimune, K. W. Chi, P. S. Mukherjee, *Chem. - Eur. J.* **2017**, *23*, 15704; e) Y. Sekine, M. Nihei, H. Oshio, *Chem. - Eur. J.* **2017**, *23*, 5193.
- [9] a) C. C. Johansson Seechurn, M. O. Kitching, T. J. Colacot, V. Snieckus, *Angew. Chem. Int. Ed.* **2012**, *51*, 5062; b) Y.-L. Ren, B. Wang, X.-Z. Tian, S. Zhao, J. Wang, *Tetrahedron Lett.* **2015**, *56*, 6452; c) J. He, M. Wasa, K. S. L. Chan, Q. Shao, J.-Q. Yu, *Chem. Rev.* **2017**, *117*, 8754; d) C. Liu, Y. Liu, R. Liu, R. Lalancette, R. Szostak, M. Szostak, *Org. Lett.* **2017**, *19*, 1434.
- [10] a) R. Takise, K. Muto, J. Yamaguchi, *Chem. Soc. Rev.* **2017**, *46*, 5864; b) A. H. Dardir, P. R. Melvin, R. M. Davis, N. Hazari, M. Mohadjer Beromi, *J. Org. Chem.* **2018**, *83*, 469; c) J. Latham, E. Brandenburger, S. A. Shepherd, B. R. K. Menon, J. Micklefield, *Chem. Rev.* **2018**, *118*, 232.
- [11] a) V. A. Likholobov, V. B. Fenelonov, L. G. Okkel, O. V. Goncharova, L. B. Avdeeva, V. I. Zaikovskii, G. G. Kuvshinov, V. A. Semikolenov, V. K. Duplyakin, O. N. Baklanova, G. V. Plaksin, *React. Kinet. Mech. Cat.* **1995**, *54*, 381; b) M. Hartmann, L. Kevan, *Chem. Rev.* **1999**, *99*, 635; c) B. Chen, C. Liang, J. Yang, D. S. Contreras, Y. L. Clancy, E. B. Lobkovsky, O. M. Yaghi, S. Dai, *Angew. Chem. Int. Ed.* **2006**, *45*, 1390; d) E. C. D. Oliveira, C. T. G. V. M. T. Pires, H. O. Pastore, *J. Braz. Chem. Soc.* **2006**, *17*, 16.
- [12] a) L. Alaerts, C. E. Kirschhock, M. Maes, M. A. van der Veen, V. Finsy, A. Depla, J. A. Martens, G. V. Baron, P. A. Jacobs, J. F. Denayer, D. E. De Vos, *Angew. Chem. Int. Ed.* **2007**, *46*, 4293; b) A. U. Czaja, N. Trukhan,

FULL PAPER

- U. Muller, *Chem. Soc. Rev.* **2009**, *38*, 1284; c) V. Finsy, C. E. Kirschhock, G. Vedts, M. Maes, L. Alaerts, D. E. De Vos, G. V. Baron, J. F. Denayer, *Chem. - Eur. J.* **2009**, *15*, 7724.
- [13] a) O. K. Farha, I. Eryazici, N. C. Jeong, B. G. Hauser, C. E. Wilmer, A. A. Sarjeant, R. Q. Snurr, S. T. Nguyen, A. O. Yazaydin, J. T. Hupp, *J. Am. Chem. Soc.* **2012**, *134*, 15016; b) J. R. Li, J. Sculley, H. C. Zhou, *Chem. Rev.* **2012**, *112*, 869; c) Z. R. Herm, E. D. Bloch, J. R. Long, *Chem. Mater.* **2013**, *26*, 323; d) B. Van de Voorde, B. Bueken, J. Denayer, D. De Vos, *Chem. Soc. Rev.* **2014**, *43*, 5766; e) J. M. Holcroft, K. J. Hartlieb, P. Z. Moghadam, J. G. Bell, G. Barin, D. P. Ferris, E. D. Bloch, M. M. Algaradah, M. S. Nassar, Y. Y. Botros, K. M. Thomas, J. R. Long, R. Q. Snurr, J. F. Stoddart, *J. Am. Chem. Soc.* **2015**, *137*, 5706; f) K. J. Hartlieb, J. M. Holcroft, P. Z. Moghadam, N. A. Vermeulen, M. M. Algaradah, M. S. Nassar, Y. Y. Botros, R. Q. Snurr, J. F. Stoddart, *J. Am. Chem. Soc.* **2016**, *138*, 2292.
- [14] a) R. S. Mulliken, *J. Am. Chem. Soc.* **1950**, *72*, 600; b) J. L. Lippert, M. W. Hanna, P. J. Trotter, *J. Am. Chem. Soc.* **1969**, *91*, 4035; c) H. Adams, S. L. Cockroft, C. Guardigli, C. A. Hunter, K. R. Lawson, J. Perkins, S. E. Spey, C. J. Urch, R. Ford, *ChemBioChem* **2004**, *5*, 657; d) M. B. Shah, J. Liu, Q. Zhang, C. D. Stout, J. R. Halpert, *ACS Chem. Biol.* **2017**, *12*, 1204.
- [15] a) H. A. Torrey, W. H. Hunter, *J. Am. Chem. Soc.*, **1912**, *34*, 702; b) C. White, A. Yates, P. M. Maitlis, D. M. Heinekey, *Inorg. Synth.*, **1992**, *29*, 228; c) M. Kamaya, Y. Hamada, S. Yazaki, K. Nagashima, E. Ishii, *Anal. Chim. Acta*, **1992**, *264*, 131.

FULL PAPER

Entry for the Table of Contents (Please choose one layout)

Layout 1:

FULL PAPER

Ag- π interactions and steric effects: two stable Rh^{III}/Ag^I mixed macrocages have been obtained following a multistep procedure and the exploration of cage in the separation of dihalogenated benzene derivatives with high selectivity.



H.-N. Zhang, Y. Lu, W.-X. Gao, Y.-J. Lin, G.-X. Jin*

Page No. – Page No.

Selective encapsulation and separation of dihalobenzene isomers with discrete heterometallic macrocages

Layout 2:

FULL PAPER

((Insert TOC Graphic here; max. width: 11.5 cm; max. height: 2.5 cm))

Author(s), Corresponding Author(s)*

Page No. – Page No.

Title

Text for Table of Contents